Avicenna Journal of Phytomedicine (AJP)

Short-Communication

Urolithin A in cardiomyocyte protection: modulating autophagy and apoptosis in ischemia-reperfusion injury

Mohammad Ebrahim Astaneh[1,2,3], Ali Ghanbariasad[4], Razie Ranjbar[4], Amirhossein Sahebkar[5,6,7], Narges Fereydouni[8,*]

[1]*Department of Anatomical Sciences, School of Medicine, Fasa University of Medical Sciences, Fasa, Iran*
[2]*Department of Tissue Engineering, School of Medicine, Fasa University of Medical Sciences, Fasa, Iran*
[3] *Student Research Committee, Fasa University of Medical Sciences, Fasa, Iran*
[4]*Department of Medical Biotechnology, School of Medicine, Fasa University of Medical Sciences, Fasa, Iran*
[5]*Center for Global Health Research, Saveetha Medical College and Hospitals, Saveetha Institute of Medical and Technical Sciences, Saveetha University, Chennai, India*
[6]*Biotechnology Research Center, Pharmaceutical Technology Institute, Mashhad University of Medical Sciences, Mashhad, Iran*
[7]*Applied Biomedical Research Center, Mashhad University of Medical Sciences, Mashhad, Iran*
[8]*Noncommunicable Diseases Research Center, Fasa University of Medical Sciences, Fasa, Iran*

Article history:
Received: Nov 17, 2024
Received in revised form: Oct 07, 2025
Accepted: Oct 11, 2025
Epub ahead of print

**** Corresponding Author:***
Tel: +987153350944-6
Fax: +987153350944-6
narges.fereydouni2020@gmail.com

Keywords:
Urolithin A
Cardiomyocytes
Hypoxia–reperfusion (HR) model
Autophagy
Apoptosis
Inflammation

Abstract

Objective: Cardiovascular diseases remain a major cause of global mortality, and myocardial ischemia–reperfusion (IR) injury contributes substantially to cardiac damage. Urolithin A (UA), a gut-derived metabolite of dietary ellagitannins, regulates autophagy, apoptosis, and inflammation. This study evaluated UA in an in vitro hypoxia–reperfusion (HR) model using H9C2 cardiomyocytes.

Materials and Methods: Cell viability was assessed by MTT assay across multiple UA concentrations. Real-time PCR quantified the expression of genes associated with autophagy, apoptosis, and inflammation.

Results: UA caused concentration-dependent cytotoxicity, with greater sensitivity under normoxia (IC_{50} = 25.4 µM) than HR conditions (IC_{50} = 70.1 µM). Under HR, UA increased LC3, TFEB, LAMP2, and BECN1 expression while reducing P62, consistent with enhanced autophagic flux. Bax and BCL2 were both downregulated, and the decreased Bax/BCL2 ratio indicated a net anti-apoptotic effect. However, UA also increased IL-1β, IL-6, and TNF-α expression, demonstrating a concurrent pro-inflammatory response.

Conclusion: UA enhances autophagy and suppresses apoptosis in HR-stressed cardiomyocytes but simultaneously promotes inflammatory signaling. These context-dependent effects support its potential as a modulator of IR injury while underscoring the need for protein-level validation, dose optimization, temporal analysis, and in vivo studies before therapeutic application.

Please cite this paper as:
Astaneh M.E, Ghanbariasad A, Ranjbar R, Sahebkar A, Fereydouni N. Urolithin A in cardiomyocyte protection: modulating autophagy and apoptosis in ischemia-reperfusion injury. Avicenna J Phytomed, 2025. Epub ahead of print.

Introduction

Cardiovascular diseases (CVDs) are the leading cause of death worldwide, with myocardial ischemia–reperfusion (IR) injury playing a central role in conditions such as myocardial infarction. IR injury occurs when blood flow is restored to ischemic myocardium, paradoxically exacerbating damage through oxidative stress, inflammation, and apoptosis (He et al. 2022; Townsend et al. 2022; Zhao 2021). Autophagy, a cellular process that degrades damaged organelles and maintains homeostasis under stress, has emerged as a potential protective mechanism in IR injury (Ikeda et al. 2022; Khan and Sabatasso 2024; Ma et al. 2020; Ott et al. 2021). However, its role in cardiomyocytes is complex and sometimes contradictory, highlighting the need for further investigation to develop targeted therapeutic strategies.

Urolithin A (UA), a metabolite derived from ellagitannins present in foods such as pomegranates and berries, has shown promise due to its ability to modulate key cellular processes involved in IR injury, including autophagy, apoptosis, and inflammation (D'Amico et al. 2021; Gong et al. 2022; Li et al. 2024; Zheng et al. 2020). Previous studies have demonstrated UA protective effects in ischemic injury of the brain (Ahsan et al. 2019), kidney (Wang et al. 2019), pancreas (Zhang et al. 2021), and other tissues (Gong et al. 2022; Liu et al. 2023), primarily through regulation of autophagy, oxidative stress, and inflammatory pathways. Limited evidence also suggests beneficial effects of UA or its analogues in cardiac models (Huang et al. 2023; Tang et al. 2017).

Despite these advances, detailed studies examining how UA simultaneously regulates autophagy, apoptosis, and inflammation specifically in cardiomyocytes under hypoxia–reperfusion (HR) conditions remain scarce. The present study addresses this gap by applying an in vitro HR model in H9C2 cardiomyocytes, allowing us to dissect these interconnected pathways in response to UA exposure. This approach enables a detailed cellular-level analysis of autophagic, apoptotic, and inflammatory responses under conditions that mimic ischemia and reperfusion in vivo.

In other models of IR injury, UA has demonstrated diverse protective effects by modulating autophagy, apoptosis, and inflammation. In neuronal and renal ischemia models, UA enhanced autophagic flux, evidenced by increased expression of *LC3*, *TFEB*, *LAMP2*, and *BECN1*, alongside reduced *P62* levels, indicating elevated autophagic degradation (Ahsan et al. 2019; Wang et al. 2019; Zhang et al. 2021). UA may confer protection by modulating interconnected pathways governing autophagy (e.g., *TFEB*/CLEAR network), apoptosis (e.g., *Bax*/*BCL2* balance via PI3K/Akt signaling), and inflammation (e.g., NF-κB pathways), though their relative contributions in cardiomyocytes under HR remain unclear. In neuronal models, UA alleviated endoplasmic reticulum (ER) stress—a key mediator of apoptosis—by promoting autophagic degradation of damaged proteins and reducing pro-apoptotic signaling (Ahsan et al. 2019; Zhang et al. 2021). Anti-apoptotic effects via *Bax* downregulation and *BCL2* modulation have been observed in both neuronal and cardiac models, suggesting a conserved protective mechanism (Ahsan et al. 2019; Gong et al. 2022; Tang et al. 2017).

UA exerts diverse biological effects, particularly in modulating autophagy, apoptosis, and inflammation. In IR injury, UA has been shown to protect cardiomyocytes, neurons, and other tissues by regulating multiple molecular pathways (Ahsan et al. 2019; Gong et al. 2022; Tuohetaerbaike et al. 2020). It enhances autophagic flux, as evidenced by increased expression of *LC3*, *TFEB*, *LAMP2*, and *BECN1*, alongside reduced *p62* levels, indicating elevated autophagic degradation. Activation of the CLEAR network and increased lysosomal capacity through *TFEB* is critical for mitigating cellular

stress during ischemia (Wang et al. 2019). Additionally, UA alleviates endoplasmic reticulum (ER) stress—a key mediator of apoptosis—by promoting autophagic degradation of damaged proteins and reducing pro-apoptotic signaling, supported by decreased phosphorylated PERK levels (Ahsan et al. 2019; Zhang et al. 2021). UA also modulates apoptotic pathways during HR stress by downregulating *Bax* and regulating *BCL2* via the PI3K/Akt pathway, thereby preventing the release of pro-apoptotic factors and reducing cardiomyocyte loss. This anti-apoptotic effect, observed in both cardiomyocytes (Tang et al. 2017), and neurons (Ahsan et al. 2019; Gong et al. 2022), represents a conserved protective mechanism across tissues.

UA's effects on inflammation appear context-dependent. While many studies report anti-inflammatory effects via NF-κB inhibition and interleukin 10 (*IL-10*) upregulation in neuronal and renal models (Li et al. 2024; Wang et al. 2019), its impact in cardiomyocytes under HR is less characterized and may differ due to tissue-specific signaling. Transient pro-inflammatory responses during ischemic stress may represent adaptive 'protective inflammation' facilitating damaged cell clearance and tissue repair, as autophagy itself can modulate NF-κB activity (Dong et al. 2022; Mo et al. 2020).

Accordingly, this study investigates UA's modulatory effects on autophagy, apoptosis, and inflammation in H9C2 cardiomyocytes under HR conditions as a surrogate for cardiac IR injury. We hypothesized that UA would enhance autophagic flux and reduce apoptosis under HR stress. Given the context-dependent nature of its effects across different tissues and injury models, we further sought to characterize inflammatory signaling responses, which may represent either detrimental activation or transient, protective inflammation. By evaluating cell viability and gene expression across different UA concentrations, this work aims to elucidate the complex interactions of UA with cellular stress pathways in cardiomyocytes, offering insights into its potential as a therapeutic agent for cardiac IR injury.

Materials and Methods

Experimental groups and treatment protocols

Four experimental groups were established to investigate the effects of Urolithin A (UA, ≥97% HPLC grade, Sigma Aldrich, USA) at varying concentrations (Table 1). The control group was cultured in high-glucose DMEM (Sigma Aldrich, USA) for 24 hours at 37°C with 5% CO_2. The hypoxia–reperfusion (HR) group was pre-incubated for 18 hours in low-glucose DMEM (1 g/L glucose, Sigma Aldrich, USA) at 37°C with 5% CO_2, then subjected to hypoxia (1% O_2, 94% N_2, 5% CO_2) for 3 hours in a modular incubator chamber (Billups-Rothenberg Inc., USA), verified by an oxygen sensor (Pyroscience FireSting O_2, Germany), followed by reoxygenation for 3 hours under normoxic conditions (21% O_2, 5% CO_2) in fresh low-glucose DMEM at 37°C. The HR + UA group followed the identical protocol with UA added at the initiation of the 18-hour pre-incubation period and maintained throughout the entire 24-hour experimental duration (18h pre-incubation + 3h hypoxia + 3h reoxygenation). The UA group was cultured for 24 hours in high-glucose DMEM supplemented with UA under normoxic conditions. UA was tested at concentrations of 0, 1.56, 3.125, 6.25, 12.5, 25, 50, and 100 µM under both normal and HR conditions. Experimental procedures and concentration ranges were based on previous studies (Tang et al. 2017; Zheng et al. 2020). All protocols were approved by the Bioethics Committee of Fasa University of Medical Sciences (Ethics code: IR.FUMS.REC.1401.102). UA was tested at concentrations of 0, 1.56, 3.125, 6.25, 12.5, 25, 50, and 100 µM under both normal and HR conditions.

Table 1. Experimental conditions for control, hypoxia-reperfusion (HR), and UA treatment groups

Groups	Experimental setup
1. Control	24 hr, 37°C, 5% CO_2 in High DMEM
2. HR	Step 1. 18 hr, 37°C, 5% CO_2 in Low DMEM
	Step 2. 3 hr in hypoxia conditions, 37°C, 5% CO_2 in Low DMEM
	Step 3. 3 hr, 37°C, 5% CO_2 in Low DMEM
3. HR+ UA	Step 1. 18 hr, 37°C, 5% CO_2 in Low DMEM with UA
	Step 2. 3 hr in hypoxia, 37°C, 5% CO_2 in Low DMEM with UA
	Step 3. 3 hr, 37°C, 5% CO_2 in Low DMEM with UA
4. UA	24 hr, 37°C, 5% CO_2 in High DMEM with UA

HR: Hypoxia-reperfusion, UA: Urolithin A, DMEM: Dulbecco's modified eagle medium

Cell culture and cytotoxicity assessment

H9C2 rat cardiomyoblast cells (Pasteur Institute of Iran) at passages 8-15 were cultured in high-glucose Dulbecco's Modified Eagle Medium (DMEM, Sigma Aldrich, USA) supplemented with 10% fetal bovine serum (FBS, Gibco, USA) and 1% penicillin-streptomycin (100 U/mL penicillin, 100 µg/mL streptomycin; Sigma Aldrich, USA) at 37°C in a humidified atmosphere with 5% CO_2. For hypoxia induction, cells were placed in a modular incubator chamber (Billups-Rothenberg Inc., USA) flushed with a certified gas mixture (1% O_2, 94% N_2, 5% CO_2) for 3 hours. Oxygen concentration was continuously monitored and verified using an oxygen sensor (Pyroscience FireSting O_2, Germany) to ensure stable hypoxic conditions throughout the exposure period.

Cytotoxicity was assessed using the MTT [3-(4,5-dimethylthiazol-2-yl)-2,5-diphenyltetrazolium bromide] assay. Cells were seeded at 5,000 cells/well in 96-well plates and allowed to adhere for 24 hours before treatment with UA (0, 1.56, 3.125, 6.25, 12.5, 25, 50, and 100 µM) for 24 hours. Following treatment, 20 µL of MTT solution (5 mg/mL, Sigma Aldrich, USA) was added to each well and incubated for 4 hours at 37°C. Formazan crystals were dissolved in 150 µL dimethyl sulfoxide (DMSO, >99.7% purity, Dr. Mojallali, Iran), and absorbance was measured at 570 nm using a microplate reader (Epoch, BioTek, USA). Each concentration was tested in six technical replicates per experiment, and experiments were repeated three times independently (n=3 biological replicates), resulting in 18 data points per concentration. Cell viability was calculated as a percentage relative to vehicle-treated control wells. IC_{50} values were determined using nonlinear regression analysis with a four-parameter logistic curve [log(inhibitor) vs. response – variable slope] in GraphPad Prism 6 software.

Real-time PCR analysis

Following IC_{50} determination, cells were treated with UA at the IC_{50} concentration under normal and HR conditions for gene expression analysis. Real-time PCR was conducted to evaluate the expression of genes associated with autophagy (*LC3*, *TFEB*, *LAMP2*, *BECN1*, *P62*), apoptosis (*Bax*, *BCL2*), and inflammation (*TNF-α*, *IL-6*, *IL-1β*). Total RNA was extracted using the Trizol RNA extraction kit (Yektatajhiz, Iran) according to the manufacturer's protocol and quantified with a spectrophotometer (CE9500, CECIL, UK). RNA purity was confirmed by A260/A280 ratios between 1.8-2.0. One microgram of RNA was reverse transcribed into cDNA using a reverse transcription kit (Yektatajhiz, Iran). Real-time PCR was performed using SYBR Green master mix (Qiagen, Germany) on a StepOnePlus qPCR system (Applied Biosystems, USA) with gene-specific primers (Pishgam Company, Iran) listed in

Table 2. The thermal cycling protocol consisted of initial denaturation at 95°C for 10 minutes, followed by 40 cycles of denaturation (95°C for 15 seconds), annealing (60°C for 30 seconds), and extension (72°C for 30 seconds). Primer specificity was confirmed by melt curve analysis demonstrating single melting peaks for each primer pair, and amplification products were verified by 2% agarose gel electrophoresis showing single bands of expected sizes. Gene expression was normalized to β-actin (*ACTB*) using the 2^(-ΔΔCt) method, with all samples analyzed in triplicate. Results represent transcriptional-level changes; protein-level validation is recommended to confirm functional autophagy, apoptosis, and inflammatory responses.

Statistical analysis

Statistical analyses were performed using GraphPad Prism 6. Data are presented as mean ± standard deviation (SD). Group comparisons were conducted using one-way ANOVA, followed by Tukey's *post hoc* test. A p-value <0.05 was considered statistically significant. All experiments were performed in triplicate to ensure reproducibility, and IC_{50} values were calculated using nonlinear regression analysis.

Table 2. Forward and reverse primers used for gene expression analysis in H9C2 cells

Gene	Sequence
LC3	F: AGGAGATCTCGCAGGCCTATTA
	R: TCTCTTCCACCATCTGCCAAAG
TFEB	F: TGCTACACATCAGCTCCAATCC
	R: GCGTGTTAGGCATCTGCATTTC
LAMP2	F: AATGGCTCAGCTTTCCATGTTTC
	R: GGAAACCACCTGCTCTTTGTTG
BECN1	F: GTGTGCAGCAGTTCAAAGAAGAG
	R: CTGCCTCCAGTGTCTTCAATCT
P62	F: GCTACGAAGGCTATGAAGGCTATT
	R: GGTCCCATTCCAGTCATCTTGT
Bax	F: TGCAGACGGCAACTTCAA
	R: GATCAGCTCGGGCACTTTAG
BCL2	F: GTGGATGACTGAGTACCTGAAC
	R: GAGACAGCCAGGAGAAATCAA
IL-1β	F: CTATGGCAACTGTCCCTGAACT
	R: GGGCTTGGAAGCAATCCTTAATC
IL-6	F: GCCCTTCAGGAACAGCTATGAA
	R: TCCTCTCCGGACTTGTGAAGTA
TNF-α	F: GTGCCTCAGCCTCTTCTCATT
	R: TGGGAACTTCTCCTCCTTGTTG
ACTB	F: TGTCACCAACTGGGACGATA
	R: GGGGTGTTGAAGGTCTCAAA

LC3: Microtubule-associated protein 1 light chain 3, TFEB: Transcription factor EB, LAMP2: Lysosome-associated membrane glycoprotein 2, BECN1: Beclin 1, P62 (SQSTM1): Sequestosome 1, Bax: BCL2-associated X protein, BCL2: B-cell lymphoma 2, IL-1β: Interleukin-1 beta, IL-6: Interleukin-6, TNF-α: Tumor necrosis factor alpha, *ACTB*: β-actin (Actin beta)

Results

Cell viability

The MTT assay demonstrated that UA exerts concentration-dependent cytotoxicity on H9C2 cardiomyocytes under both normal and HR conditions (Figure 1). Under normal conditions, all tested UA concentrations (1.56–100 µM) significantly reduced cell viability compared to controls, with a half-maximal inhibitory concentration (IC_{50}) of 25.4 µM. Under HR conditions, lower UA concentrations (1.56 and 3.125 µM) did not significantly affect viability, indicating reduced cytotoxicity at these levels. In contrast, concentrations of 6.25 µM and above caused significant decreases in cell viability, with an IC_{50} of 70.1 µM—substantially higher than under normal conditions. This paradoxical reduction in UA cytotoxicity under HR stress suggests that hypoxia-reperfusion preconditioning activates endogenous protective mechanisms that confer resistance to UA-induced cell death. The adaptive stress response triggered by HR may include enhanced autophagic flux, upregulation of stress proteins, and metabolic reprogramming, collectively buffering against subsequent cytotoxic insults.

Gene expression

Real-time PCR analysis revealed that UA treatment during HR significantly upregulated autophagy-related genes, including *LC3*, *TFEB*, *LAMP2*, and *BECN1*, while downregulating *P62*, indicating enhanced autophagic activity and flux (Figure 2). Concurrently, the pro-apoptotic gene *Bax* and the anti-apoptotic gene *BCL2* were both downregulated, suggesting suppression of apoptosis in UA-treated H9C2 cells under HR stress. To clarify the net apoptotic effect, we calculated the *Bax*/*BCL2* ratio, which represents the balance between pro- and anti-apoptotic signaling. The *Bax*/*BCL2* ratio was significantly reduced in UA-treated HR cells (0.48 ± 0.06) compared to HR alone (0.82 ± 0.09, $p<0.01$), confirming net anti-apoptotic signaling despite concurrent downregulation of both genes. This indicates that UA shifts the apoptotic balance toward cell survival under HR stress. Despite these protective effects, inflammatory cytokines—including *IL-1β*, *IL-6*, and *TNF-α*—were markedly elevated in UA-treated cells under HR conditions compared to normal conditions, highlighting a context-dependent pro-inflammatory response.

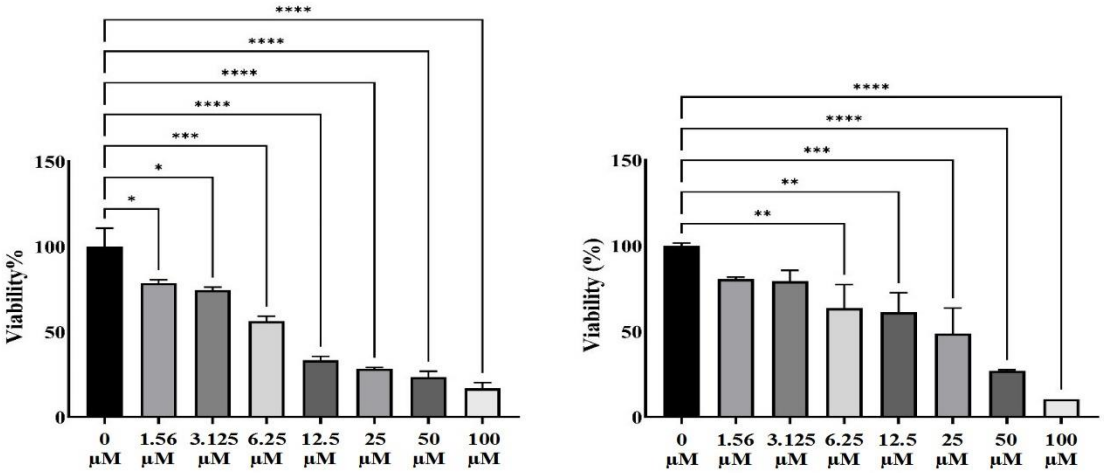

Figure 1. Viability of H9C2 cells exposed to varying concentrations of UA under (A) normal and (B) hypoxia-reoxygenation (HR) conditions for 24 hr. Data represent the mean ± SD from three independent experiments; statistical significance is indicated as *$p<0.05$, **$p<0.01$, and ***$p<0.001$.

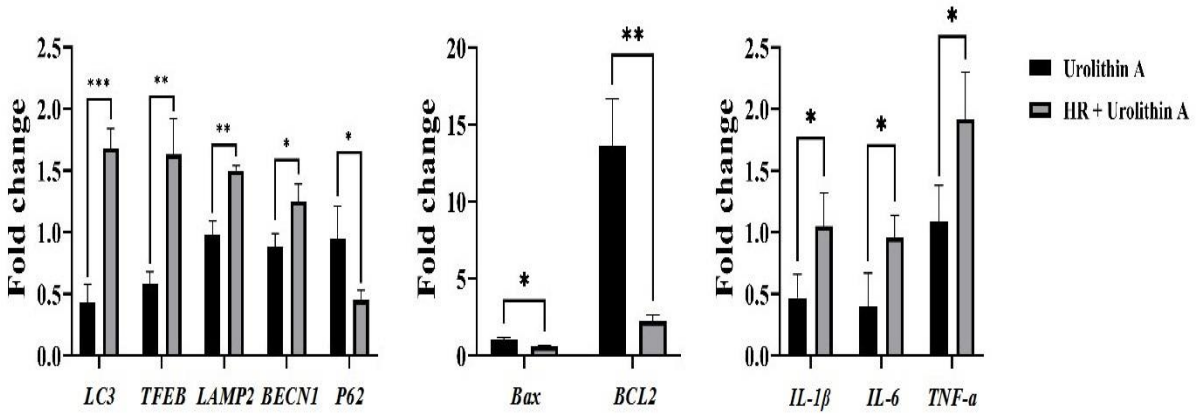

Figure 2. Expression levels of (A) autophagy markers, (B) apoptosis markers, and (C) pro-inflammatory markers in H9C2 cells subjected to normal and HR conditions for 24 hr. Data are presented as the mean ± SD from three independent experiments; statistical significance is denoted as *p < 0.05, **p < 0.01, and ***p < 0.001. HR: Hypoxia-Reperfusion, UA: Urolithin A, *LC3*: Microtubule-associated protein 1 light chain 3, *TFEB*: Transcription factor EB, *LAMP2*: Lysosome-associated membrane glycoprotein 2, *BECN1*: Beclin 1, *P62* (SQSTM1): Sequestosome 1, *Bax*: *BCL2*-associated X protein, *BCL2*: B-cell lymphoma 2, *IL-1β*: Interleukin-1 beta, *IL-6*: Interleukin-6, *TNF-α*: Tumor necrosis factor alpha, *ACTB*: β-actin (Actin beta)

Discussion

In H9C2 cardiomyocytes, urolithin A (UA) exhibited a context- and dose-dependent profile. Under normoxic conditions, UA was uniformly cytotoxic, with an IC_{50} of approximately 25.4 µM, whereas during hypoxia–reoxygenation (HR) stress, its toxicity was attenuated, with an IC_{50} of roughly 70.1 µM. The higher IC_{50} under HR conditions is a notable finding that reflects hypoxic preconditioning-induced adaptive cellular mechanisms. HR stress activates multiple protective pathways including enhanced autophagy, heat shock protein expression, HIF-1α stabilization, and metabolic adaptation toward glycolysis, which collectively confer resistance to UA-induced cytotoxicity. This phenomenon exemplifies the hormetic stress response paradigm, wherein sublethal stress exposure induces protective adaptations that enhance resilience to subsequent insults. The observation that HR stress "protects" cells from UA toxicity, rather than sensitizing them, suggests that the stress-activated survival machinery is sufficiently robust to overcome UA's cytotoxic effects at concentrations that would otherwise be lethal under normoxic conditions. Low concentrations (1.56–3.125 µM) did not significantly affect cell viability under HR conditions. At the molecular level, UA treatment during HR upregulated autophagy- and lysosome-related genes (*LC3*, *TFEB*, *LAMP2*, *BECN1*) while downregulating *P62*, consistent with enhanced autophagic flux. Concurrently, both the pro-apoptotic gene *Bax* and the anti-apoptotic gene *BCL2* were downregulated, indicating suppression of apoptotic signaling. Despite these protective effects, inflammatory cytokines (*IL-1β*, *IL-6*, *TNF-α*) were elevated relative to normoxia, reflecting a pro-inflammatory transcriptional response alongside enhanced autophagy and reduced apoptosis. While at first glance this appears contradictory, transient induction of pro-inflammatory cytokines under stress conditions may also serve adaptive roles, including activation of survival pathways, promotion of tissue remodeling, or priming for subsequent resolution phases (Ahsan et al. 2019; Gong et al. 2022; Huang et al. 2023; Li et al. 2024; Liu et al. 2023; Tang et al. 2017; Tuohetaerbaike et al. 2020; Wang et al. 2019; Zhang et al. 2021; Zheng et al. 2020). This perspective suggests that early cytokine elevation does not necessarily equate to detrimental inflammation but may represent a

compensatory mechanism in stressed cardiomyocytes.

These findings align with prior studies demonstrating that UA enhances lysosomal biogenesis and autophagic competence via the *TFEB*–CLEAR axis, increasing expression of *LAMP2* and *BECN1* and reducing *P62* (Ahsan et al. 2019; Wang et al. 2019). This reinforces UA's role as a promoter of autophagic flux under ischemic stress. The main divergence from existing literature lies in the inflammatory response: whereas many reports indicate cytokine suppression by UA in neuronal and renal IR models (Li et al. 2024; Wang et al. 2019), our HR model showed increased transcriptional expression of *IL-1β*, *IL-6*, and *TNF-α*. This apparent contradiction likely reflects multiple factors: (1) cell type-specific differences—cardiomyocytes may exhibit distinct inflammatory signaling compared to neurons or renal cells; (2) temporal dynamics—acute transcriptional upregulation in the immediate post-HR period may precede later resolution and anti-inflammatory responses; (3) model differences—isolated cardiomyocytes lack the complex interactions with immune cells, endothelial cells, and paracrine factors present in vivo, which may normally suppress or resolve inflammation; (4) dose and exposure timing differences across studies. Importantly, the concept of "protective inflammation" in ischemic injury suggests that transient cytokine elevation may serve adaptive functions including activation of survival signaling (e.g., *TNF-α*-mediated NF-κB survival pathways), promotion of cellular remodeling, and priming for subsequent anti-inflammatory resolution phases (Dong et al. 2022; Mo et al. 2020). Thus, early cytokine transcriptional induction does not necessarily indicate detrimental inflammation but may represent a compensatory stress response in HR-challenged cardiomyocytes.

UA has also been associated with modulation of the PI3K/Akt–mTOR–ULK1 pathway in ischemia/reperfusion models. Evidence suggests UA activates survival signaling and reduces apoptosis, whereas other urolithins, such as urolithin B (UB), may suppress autophagy while protecting against oxidative stress. Our data are consistent with previous findings showing enhanced autophagy and downregulation of apoptotic genes (Tang et al. 2017; Zheng et al. 2020), suggesting cytoprotection via PI3K/Akt-driven mechanisms, although protein-level confirmation is required.

The AMPK–mTOR axis provides an additional explanatory framework. UA has been shown to activate autophagy through AMPK upregulation and mTOR inhibition, thereby limiting apoptosis. Our observation of increased autophagy-related gene expression and reduced *p62*, along with *Bax* and *BCL2* downregulation, aligns with this mechanism. However, the concomitant elevation of cytokines contrasts with prior reports of anti-inflammatory effects, suggesting that acute transcriptional induction may precede later resolution (Liu et al. 2023; Zhang et al. 2021).

UA has also been implicated in mitophagy (mitochondrial selective autophagy) in other models. While our study did not directly assess mitochondrial quality control markers such as PINK1, Parkin, or mitochondrial membrane potential, our observation of *TFEB* activation and *P62* reduction suggests increased autophagic/lysosomal degradative capacity that may indirectly support mitophagy. Literature indicates that UA may favor bulk autophagy under acute ischemic stress but enhance PINK1/Parkin-mediated mitophagy under chronic metabolic stress (Ahsan et al. 2019; Huang et al. 2023). Future studies should directly measure mitochondrial quality control parameters to determine whether UA's cardioprotective effects under HR involve mitophagic clearance of damaged mitochondria.

Other studies, particularly involving urolithin B (UB), emphasize cytoprotection through Nrf2-mediated antioxidant signaling (Li et al. 2024; Zheng et al. 2020). Although we did not examine Nrf2 directly, the observed reduction in *P62* may intersect with the *P62*–Keap1–Nrf2 axis, while molecule-specific differences between UA and UB may account for mechanistic divergences across models (Li et al. 2024; Zheng et al. 2020).

In broader contexts, including diabetes and traumatic brain injury, UA has been shown to improve barrier function, reduce apoptosis, and suppress inflammatory signaling. The apparent discrepancy with our observation of elevated cytokines likely reflects the absence of immune and vascular compartments in isolated cardiomyocytes, as well as differences in timing, where early transcriptional priming precedes subsequent inflammatory resolution (Gong et al. 2022; Tuohetaerbaike et al. 2020).

Taken together, several key themes emerge. First, autophagy appears to be a unifying mechanism by which UA promotes cellular resilience, consistent with TFEB/CLEAR activation, increased *LC3*, and reduced *p62*. Second, pathway engagement is context dependent: UA consistently enhances autophagy, whereas UB often signals via Nrf2-mediated antioxidant pathways. Third, inflammatory responses are highly model- and time-dependent, with the cytokine induction observed here likely reflecting acute transcriptional activation rather than a sustained pro-inflammatory state. Fourth, viability data highlight a hormetic response, in which low-to-moderate UA doses improve survival under stress, whereas higher concentrations or normoxic exposure are cytotoxic. Finally, downregulation of both *Bax* and *BCL2* indicates general dampening of apoptotic machinery, though protein-level assays are necessary to confirm these effects.

Future studies should include protein-level validation of autophagy, apoptosis, and signaling pathways; longitudinal analyses to distinguish early versus late inflammatory responses; and direct comparisons between UA and UB to clarify molecule-specific mechanisms. Assessment of mitophagic flux and precise mapping of therapeutic concentration ranges are also warranted to optimize UA as a cardioprotective intervention. Important study limitations include: (1) reliance on transcriptional (mRNA) rather than protein-level data—Western blot analysis of *LC3-II/LC3-I* ratios and *P62* degradation would provide functional confirmation of autophagic flux; ELISA quantification of secreted *IL-1β*, *IL-6*, and *TNF-α* would verify the pro-inflammatory response; and caspase-3/7 activity assays or Annexin V/PI flow cytometry would functionally validate apoptosis suppression; (2) use of an isolated cardiomyocyte model lacking immune cell interactions and vascular components present in vivo; (3) examination of a single time point (24 hours) which cannot capture temporal dynamics of inflammatory resolution; (4) absence of in vivo validation in animal IR models. These limitations should be addressed in future investigations. In conclusion, our findings reinforce that UA enhances autophagic competence and constrains apoptosis in stressed cardiomyocytes, while emphasizing dose-dependent and temporal complexities. Context-dependent inflammatory responses highlight the need for pathway- and time-resolved studies to fully elucidate UA's therapeutic potential.

Urolithin A (UA) exhibited context- and dose-dependent effects in H9C2 cardiomyocytes, displaying cytotoxicity under normoxia but reduced toxicity during hypoxia–reoxygenation (HR). At low concentrations, UA preserved cell viability, enhanced autophagic flux—evidenced by upregulation of *LC3*, *TFEB*, *LAMP2*, and *BECN1* with concomitant

reduction of *p62*—and suppressed apoptosis via downregulation of *Bax* and *BCL2*. These protective effects were accompanied by increased inflammatory cytokine expression, indicating complex, time-dependent responses. Overall, UA promotes autophagy and limits apoptosis under HR stress, although its benefits are modulated by dose and associated inflammatory activation. Future studies should validate these mechanisms at the protein level, investigate temporal dynamics of inflammation, and define therapeutic concentration ranges to clarify UA cardioprotective potential.

Acknowledgment

We would like to express our sincere gratitude to the authors of this paper for their generous and dedicated collaboration, which has been invaluable to the successful completion of this work.

Conflicts of interest

The authors declare no competing interests.

References

Ahsan A, Zheng YR, Wu XL, et al. (2019) Urolithin A-activated autophagy but not mitophagy protects against ischemic neuronal injury by inhibiting ER stress in vitro and in vivo. CNS Neurosci Ther 25(9):976-986 doi:10.1111/cns.13136

D'Amico D, Andreux PA, Valdés P, Singh A, Rinsch C, Auwerx J (2021) Impact of the natural compound urolithin A on health, disease, and aging. Trends Mol Med 27(7):687-699 doi:10.1016/j.molmed.2021.04.009

Dong P, Liu K, Han H (2022) The role of NF-κB in myocardial ischemia/reperfusion injury. Curr Protein Pept Sci 23(8):535-547 doi:10.2174/1389203723666220817085941

Gong Q-Y, Cai L, Jing Y, et al. (2022) Urolithin A alleviates blood-brain barrier disruption and attenuates neuronal apoptosis following traumatic brain injury in mice. Neural Regen Res 17(9):2007-2013 doi:10.4103/1673-5374.335163

He J, Liu D, Zhao L, et al. (2022) Myocardial ischemia/reperfusion injury: Mechanisms of injury and implications for management. Exp Ther Med 23(6):1-11 doi:10.3892/etm.2022.11357

Huang JR, Zhang MH, Chen YJ, et al. (2023) Urolithin A ameliorates obesity-induced metabolic cardiomyopathy in mice via mitophagy activation. Acta pharmacologica Sinica 44(2):321-331 doi:10.1038/s41401-022-00919-1

Ikeda S, Zablocki D, Sadoshima J (2022) The role of autophagy in death of cardiomyocytes. J Mol Cell Cardiol 165:1-8 doi:10.1016/j.yjmcc.2021.12.006

Khan AA, Sabatasso S (2024) Autophagy in myocardial ischemia and ischemia/reperfusion. Cardiovasc Pathol 74:107691 doi:10.1016/j.carpath.2024.107691

Li Z-w, Tang H, Chen X-x, et al. (2024) Urolithin B Attenuates Cerebral Ischemia–reperfusion Injury by Modulating Nrf2-regulated Anti-oxidation in Rats. Neuroscience 538:46-58 doi:10.1016/j.neuroscience.2023.11.002

Liu M, Chen Z, Zhang H, et al. (2023) Urolithin A alleviates early brain injury after subarachnoid hemorrhage by regulating the AMPK/mTOR pathway-mediated autophagy. Neuro-Chirurgie 69(5):101480 doi:10.1016/j.neuchi.2023.101480

Ma W, Wei S, Zhang B, Li W (2020) Molecular mechanisms of cardiomyocyte death in drug-induced cardiotoxicity. Front Cell Dev Biol 8:434 doi:10.3389/fcell.2020.00434

Mo Y, Sun Y-Y, Liu K-Y (2020) Autophagy and inflammation in ischemic stroke. Neural Regen Res 15(8):1388-1396 doi:10.4103/1673-5374.274331

Ott C, Jung T, Brix S, et al. (2021) Hypertrophy-reduced autophagy causes cardiac dysfunction by directly impacting cardiomyocyte contractility. Cells 10(4):805 doi:10.3390/cells10040805

Tang L, Mo Y, Li Y, et al. (2017) Urolithin A alleviates myocardial ischemia/reperfusion injury via PI3K/Akt pathway. Biochem Biophys Res Commun 486(3):774-780 doi:10.1016/j.bbrc.2017.03.119

Townsend N, Kazakiewicz D, Lucy Wright F, et al. (2022) Epidemiology of cardiovascular disease in Europe. Nat Rev

Cardiol 19(2):133-143 doi:10.1038/s41569-021-00607-3

Tuohetaerbaike B, Zhang Y, Tian Y, et al. (2020) Pancreas protective effects of Urolithin A on type 2 diabetic mice induced by high fat and streptozotocin via regulating autophagy and AKT/mTOR signaling pathway. J Ethnopharmacol 250:112479 doi:10.1016/j.jep.2019.112479

Wang Y, Huang H, Jin Y, et al. (2019) Role of TFEB in autophagic modulation of ischemia reperfusion injury in mice kidney and protection by urolithin A. Food Chem Toxicol 131:110591 doi:10.1016/j.fct.2019.110591

Zhang Y, Aisker G, Dong H, Halemahebai G, Zhang Y, Tian L (2021) Urolithin A suppresses glucolipotoxicity-induced ER stress and TXNIP/NLRP3/IL-1β inflammation signal in pancreatic β cells by regulating AMPK and autophagy. Phytomedicine 93:153741 doi:10.1016/j.phymed.2021.153741

Zhao D (2021) Epidemiological features of cardiovascular disease in Asia. JACC Asia 1(1):1-13 doi:10.1016/j.jacasi.2021.04.007

Zheng D, Liu Z, Zhou Y, et al. (2020) Urolithin B, a gut microbiota metabolite, protects against myocardial ischemia/reperfusion injury via p62/Keap1/Nrf2 signaling pathway. Pharmacol Res 153:104655 doi:10.1016/j.phrs.2020.104655